NANOPARTICLES

Molecular ligand modulation of palladium nanocatalysts for highly efficient and robust heterogeneous oxidation of cyclohexenone to phenol

Teng Xue,[1]* Zhaoyang Lin,[2]* Chin-Yi Chiu,[1] Yongjia Li,[1] Lingyan Ruan,[1] Gongming Wang,[2] Zipeng Zhao,[1] Chain Lee,[2] Xiangfeng Duan,[2,3†] Yu Huang[1,3†]

Metallic nanoparticles are emerging as an exciting class of heterogeneous catalysts with the potential advantages of exceptional activity, stability, recyclability, and easier separation than homogeneous catalysts. The traditional colloid nanoparticle syntheses usually involve strong surface binding ligands that could passivate the surface active sites and result in poor catalytic activity. The subsequent removal of surface ligands could reactivate the surface but often leads to metal ion leaching and/or severe Ostwald ripening with diminished catalytic activity or poor stability. Molecular ligand engineering represents a powerful strategy for the design of homogeneous molecular catalysts but is insufficiently explored for nanoparticle catalysts to date. We report a systematic investigation on molecular ligand modulation of palladium (Pd) nanoparticle catalysts. Our studies show that β-functional groups of butyric acid ligand on Pd nanoparticles can significantly modulate the catalytic reaction process to modify the catalytic activity and stability for important aerobic reactions. With a β-hydroxybutyric acid ligand, the Pd nanoparticle catalysts exhibit exceptional catalytic activity and stability with an unsaturated turnover number (TON) >3000 for dehydrogenative oxidation of cyclohexenone to phenol, greatly exceeding that of homogeneous Pd(II) catalysts (TON, ~30). This study presents a systematic investigation of molecular ligand modulation of nanoparticle catalysts and could open up a new pathway toward the design and construction of highly efficient and robust heterogeneous catalysts through molecular ligand engineering.

INTRODUCTION

Heterogeneous nanoparticle catalysts are a topic of increasing interest due to their long-term stability, recyclability, and easier separation from the reaction mixture (*1*–*4*). Molecular ligands play an essential role in the design of homogeneous molecular catalysts, where the molecular ligands can be used to tune the catalytic activity, selectivity, versatility, and stability. On the other hand, the impact of molecular ligands on nanoparticle catalysts is far less understood. To date, most efforts have been limited to exploring the roles of molecular ligands in controlling the size and the facet of nanoparticles during nanoparticle synthetic steps (*5*–*9*). A few examples have suggested that a local ligand-induced microenvironment could enhance the catalytic activity by bringing the catalyst and the substrate into close proximity (*10*) or facilitate asymmetric reactions due to ligand chirality (*11*). Systematic ligand engineering studies are rarely reported toward nanoparticle catalysts simultaneously with enhanced catalytic activity and stability, especially for industry-relevant reactions. Here, we report a systematic study of heterogeneous Pd nanoparticle catalysts for aerobic oxidation reactions, especially phenol production.

Aerobic oxidation reactions have attracted significant industrial attention because of their mild and green conditions. Homogenous Pd catalysts have proved successful in driving these reactions. However, the inevitable deligation processes during the aerobic oxidation cycles can lead to the formation of inactive Pd black and deactivate the catalysts (Fig. 1) (*12*–*14*). Phenols are recognized as the key structure motif and core building block for a wide range of industrial chemicals (*15*). The selective functionalization of phenols is generally challenging. Electrophilic substitution represents the most common method for the synthesis of a variety of para- and ortho-substituted phenols but is not applicable for meta-substituted phenols. Dehydrogenation of cyclohexanones followed by tautomerization can result in meta-substituted phenols but is often limited by relatively low turnover, harsh reaction conditions, poor functional group tolerance, and the requirement of additional sacrificial agents (*16*–*20*). The Stahl group has recently developed a homogeneous Pd(II)-catalyzed aerobic oxidation method to enable a high-yield transformation of cyclohexenone to phenol under relatively mild reaction conditions using only oxygen as the oxidant (*21*). However, like other aerobic oxidation reactions, the deligation from homogeneous Pd catalysts results in catalytically inactive large Pd particles (>100 nm), leading to untimely deactivation of catalytic activity and a relatively low turnover number (TON; ~30) (*22*, *23*). Studies have shown that heterogeneous Pd/C catalysts can catalyze dehydrogenation reactions; however, the reactions require a high catalyst/reactant ratio, an addition of hydrogen acceptors, a long reaction time, and an elevated temperature (*24*–*26*). Heterogeneous Pd nanoparticles on different supports have also been explored for oxidative dehydrogenation of cyclohexenones but typically with extremely low yield (<1.5%) (*21*).

RESULTS AND DISCUSSION

Here, we report a rational design and systematic investigation of the ligand effect on Pd nanoparticle catalysts for aerobic oxidation, especially oxidation of cyclohexenone to phenol, using variable β-substituted butyric acid as the capping ligands. Our studies show that β-hydroxybutyric acid (HB) can function as a particularly unique molecular ligand for Pd nanoparticles with excellent catalytic activity and stability and can be used to catalyze the dehydrogenative oxidation of cyclohexenone to phenol with an unsaturated TON >3000, greatly exceeding that of the homogeneous Pd(II) catalysts (TON, ~30). Further kinetic studies also demonstrated that β-functional groups of butyric acids can actively participate in the catalytic cycle to mediate the nanocatalyst activity and stability.

[1]Department of Materials Science and Engineering, University of California Los Angeles, Los Angeles, CA 90095, USA. [2]Department of Chemistry and Biochemistry, University of California Los Angeles, Los Angeles, CA 90095, USA. [3]California NanoSystems Institute, University of California Los Angeles, Los Angeles, CA 90095, USA.
*These authors contributed equally to this work.
†Corresponding author. Email: xduan@chem.ucla.edu (X.D.); yhuang@seas.ucla.edu (Y.H.)

It has been recently shown that the homogeneous catalyst $Pd(TFA)_2$ could catalyze aerobic dehydrogenative oxidation of cyclohexenone to phenol with a moderate yield (*21*). Acids are released during the cyclohexenone-to-phenol transformation processes and then reenter the catalytic cycle to regenerate catalytic active Pd(II) species. The substitution of homogeneous Pd catalysts with ultrafine Pd nanostructures can also catalyze the reaction but requires additional acid activation. Our initial studies on commercial Pd/C showed nearly no activity without acid (yield, <1%), consistent with previous studies (*21*). The addition of weak acetic acid (HOAc) could slightly increase the yield (6%), whereas the introduction of a strong acid, trifluoroacetic acid (TFA), could boost the yield to 67%. However, the carbon black–supported Pd nanoparticles undergo a severe Ostwald ripening process during the reaction to form large inactive particles with essentially no recyclability (yield, <1% for the recycled Pd/C catalysts).

The severe ripening issue of the commercial Pd/C could be attributed to the fact that Pd nanoparticles do not have a proper ligand environment to protect them from leaching off Pd(II) ions during the catalytic cycles. The use of ligands with a strong binding functional group could ensure nanoparticle stability but often severely compromises the catalytic activity because of the passivation of the catalytic active sites by the strong binding ligands (*27*). Therefore, it is a considerable challenge to design a proper surface ligand that can maintain nanoparticle stability without sacrificing the catalytic activity. To this end, we propose using butyric acid with variable β-substitution as the secondary binding site to engineer the particle stability. Instead of engineering the primary binding functional group that could fundamentally change the nanoparticle size/morphology or directly passivate the catalytic active sites, the β-functional groups can function as secondary binding sites to capture/retain the leached Pd(II) ions near the nanoparticle surface and regulate their participation in the catalytic cycle without significantly altering the binding conditions to the nanoparticle surfaces (*28*). The Pd nanoparticles were synthesized with a diameter of 10 nm using HB as the capping agent, following a process that we recently developed for the synthesis of Pt nanoparticles (*29*). The particle synthesis was conducted in aqueous solutions containing Na_2PdCl_4, ascorbic acid, and $NaBH_4$. Fourier transform infrared (FTIR) studies confirm that the carboxylic group strongly binds to the Pd surfaces, whereas the β-hydroxy group only weakly interacts with the Pd surfaces (see fig. S1).

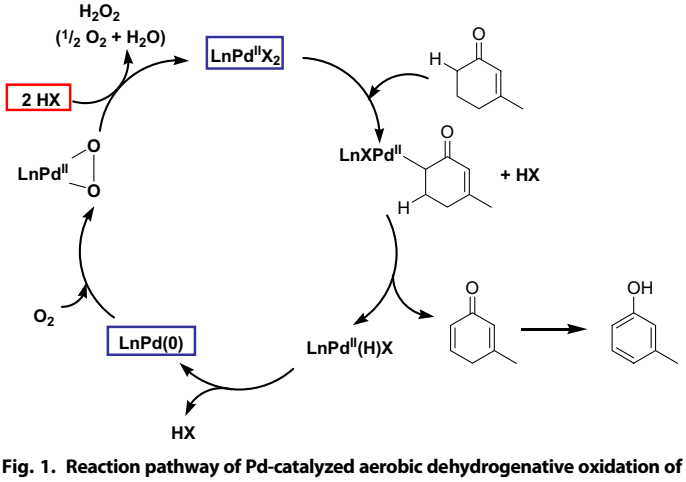

Fig. 1. Reaction pathway of Pd-catalyzed aerobic dehydrogenative oxidation of cyclohexenone to phenol. Ln represents the various β-substituted butyric acid ligands. HX represents the acids added to the reaction.

The resulting nanoparticles were supported on carbon black and used as the catalysts [3-hydroxybutyric acid–ligated Pd nanoparticles (HB-Pd/C)] for aerobic oxidation of cyclohexenone to phenol, which is compared with the catalytic behavior of the homogeneous catalyst $Pd(TFA)_2$. Under the reaction conditions of various substrate/catalyst ratios, the TON normalized by the total amount of Pd catalyst has been determined. TON is an important measure of catalyst stability. Under low turnover conditions, namely, low substrate/catalyst ratio (100:3), the TON of the heterogeneous nanoparticle catalyst HB-Pd/C is 31, about 1.5 times higher than that of the homogeneous $Pd(TFA)_2$ catalyst (20) after a 24-hour reaction (Table 1). HB-Pd/C also showed a maximum turnover frequency (TOF) of around 4.33 $hour^{-1}$, higher than that of $Pd(TFA)_2$ (around 2.34 $hour^{-1}$). The maximum TOF is a characterization of the intrinsic catalytic activity under a given reaction condition, regardless of the reaction rate decrease toward the end of the reaction caused by the depletion of a substrate concentration. It is important to note that calculations of both the TON and the TOF are based on the total number of Pd atoms, although there are only <10% Pd surface atoms that may function as the potential active sites for the 10-nm-size Pd nanoparticles. In contrast, in the case of $Pd(TFA)_2$ homogeneous catalysts, all Pd atoms could serve as catalytic centers. Therefore, HB-Pd/C is at least 20 times more active than $Pd(TFA)_2$ if we only consider the surface Pd atoms. Additionally, the homogeneous catalysts suffer from the competing deligation process that leads to the formation of large inactive Pd black and thus prematurely deactivate the catalytic activity with relatively low TONs. This competition reaction can be greatly accelerated under conditions of a high substrate/catalyst ratio (*30*, *31*), which inevitably limit the potential applications of homogeneous catalysts under industrial-favored high turnover conditions. For example, with an increased substrate/catalyst ratio of 1000:3, the reaction with the homogeneous $Pd(TFA)_2$ catalysts quickly saturates with a maximum yield of 8.4% and a TON of 28, indicating the deactivation of the catalyst at a low TON. The loss of catalytic activity of $Pd(TFA)_2$ is due to the formation and precipitation of large inactive Pd black particles in the reaction process (see fig. S2). In contrast, with a proper ligand environment, HB-Pd/C could drive the reaction to near completion with a yield of 95.4% and a TON of 314 (Table 1). It is important to note that the TON is unsaturated, indicating that the reaction rate is not limited by the intrinsic stability of the catalysts but only by the amount of available substrate. Further increasing the substrate/catalyst ratio to 10,000:3, the reaction with HB-Pd/C exhibits a linear time course with an unsaturated TON >3000 toward the end of the reaction (Table 1). These studies clearly demonstrate that the exceptional catalytic activity and stability of HB-Pd/C are largely retained throughout the reaction process (Fig. 2). However, we see little cyclohexanone oxidation under the same condition of cyclohexenone oxidation with either commercial Pd/C catalysts (yield, <1%) or HB-Pd/C catalysts (yield, <3%). These results are consistent

Table 1. The TON of heterogeneous catalyst HB-Pd/C and homogeneous catalyst $Pd(TFA)_2$ under different reaction conditions. Under a low turnover condition, the substrate/catalyst ratio is 100:3; under a high turnover condition, the substrate/catalyst ratio is 1000:3; and under an ultrahigh turnover condition, the substrate/catalyst ratio is 10,000:3.

Entry	Catalyst	Low turnover	High turnover	Ultrahigh turnover
1	HB-Pd/C	31	314	>3000 (linear)
2	$Pd(TFA)_2$	20	28	—

with those of previous studies (*23*), and might be due to the change of redox potential of the Pd(0)/Pd(II) couple when interacting with different substrates.

To further understand the function of ligand β-functional groups, we synthesized nanoparticles using a series of butyric acid ligands with different β-functional groups and supported on carbon black for subsequent catalytic studies [HB-Pd/C, AB-Pd/C (3-aminobutyric acid–ligated Pd nanoparticles), and CB-Pd/C (3-chlorobutyric acid–ligated Pd nanoparticles)]. In general, all three types of Pd nanoparticles show a similar average size of 10 nm (Fig. 3, A to C). The similarity in particle size with different β-substituted ligands confirms that the carboxylic group is the primary binding site and dominates the binding affinity with Pd(0) at the particle surfaces, whereas β-functional groups (hydroxy, amino, and chloro) do not significantly alter the binding conditions to the nanoparticle surface.

We then investigated the catalytic behavior of various carbon-supported Pd nanoparticles for aerobic dehydrogenative oxidation of cyclohexenones under TFA-acidified conditions for 24 hours. The size of the Pd nanoparticles before and after catalyzing the reaction was also evaluated using a transmission electron microscope (TEM). The catalytic studies show that the HB-Pd/C–catalyzed reaction exhibits a rather high yield up to 93% (Table 2, entry 1), much higher than the commercial Pd/C. The reactions also demonstrate good heterogeneity by hot filtration test (see fig. S3), consistent with the recent finding that 3-methylcyclohexenone dehydrogenative oxidation is dominated by heterogeneous Pd nanoparticles (*23*). TEM studies show that the size of Pd nanoparticles does not exhibit any obvious change after the 24-hour reaction (Fig. 3, A and E). This is in stark contrast to commercial Pd/C catalysts that showed a severe ripening process and an increase in the particle size (Fig. 3, D and H) and diminished catalytic activity in the reharvested material (Table 2, entry 4). With the size of the HB-Pd/C largely maintained during the catalytic cycle, the reharvested HB-Pd/C displays a highly similar catalytic activity with a yield of 83% (Table 2, entry 1). The small decrease in the reaction yield may be partly attributed to the incomplete reharvest of all catalyst nanoparticles and also probably the inevitable equilibrium amount of Pd(II) species in the reaction solution (in equilibrium with ligated Pd nanoparticles) that cannot be reharvested. HB-Pd/C can also catalyze the reaction in other polar solvents such as *N*-methylpyrrolidone with a high yield (81%); however, the yield in nonpolar solvents such as hexane is low (17%), consistent with the results of homogeneous catalysts (*21*). The AB-Pd/C-catalyzed reaction shows a lower yield of 74% that greatly reduces to 24% in reactions with the recycled AB-Pd/C (Table 2, entry 2). The severe decrease of catalytic activity in the reharvested catalyst may be attributed to obvious Ostwald

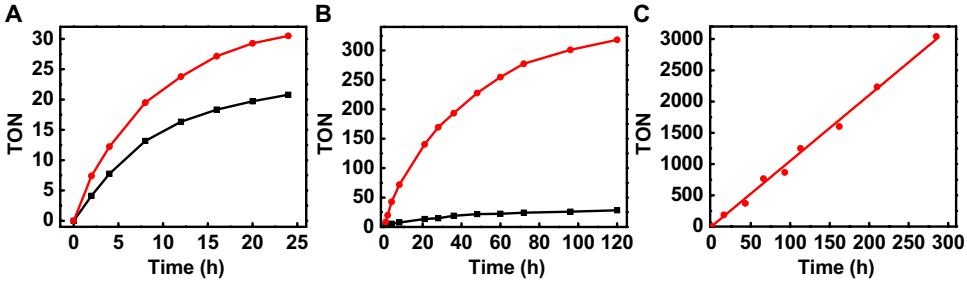

Fig. 2. Comparison of TON of heterogeneous nanoparticle catalysts with homogeneous molecular catalysts. TON of time-dependent reaction catalyzed by HB-Pd/C (red line) and $Pd(TFA)_2$ (black line) with different substrate/catalyst ratios of (**A**) 100:3, (**B**) 1000:3, and (**C**) 10,000:3.

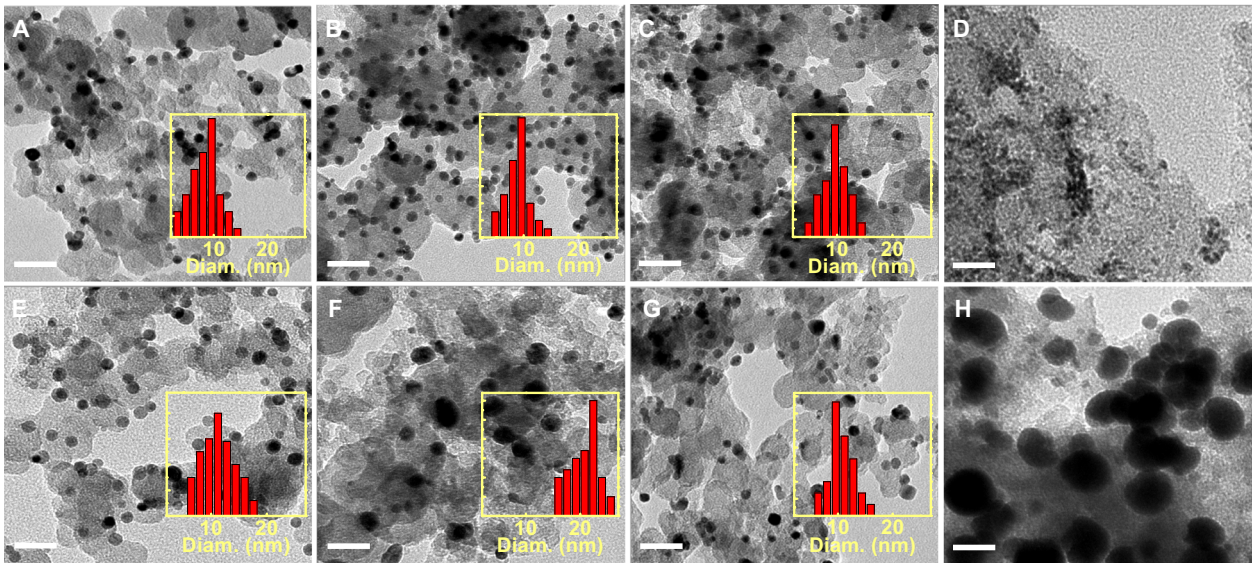

Fig. 3. TEM morphology and size distribution of HB-Pd/C, AB-Pd/C, CB-Pd/C, and commercial Pd/C. TEM morphology of (**A**) as-synthesized HB-Pd/C, (**B**) as-synthesized AB-Pd/C, (**C**) as-synthesized CB-Pd/C, (**D**) commercial Pd/C, (**E**) HB-Pd/C after 24-hour reaction, (**F**) AB-Pd/C after 24-hour reaction, (**G**) CB-Pd/C after 24-hour reaction, and (**H**) commercial Pd/C after 24-hour reaction. Scale bars, 40 nm. Inset histograms represent the size distribution of the corresponding samples.

ripening of AB-Pd nanoparticles during the catalytic cycle, with the average size increasing from 10 to 24 nm after the first cycle of reaction (Fig. 3, B and F). The CB-Pd/C–catalyzed reaction exhibits an even lower initial yield of 57% in its first cycle, which is, however, largely retained (48%) in the reharvested catalysts (Table 2, entry 3). The average size of the CB-Pd/C nanoparticles is largely unchanged after catalyzing the reactions (Fig. 3, C and G).

We have further investigated the reaction kinetics by monitoring the product yield as a function of reaction time, based on which we can determine the maximum TOF of each catalyst normalized by the total number of Pd atoms in the catalyst. The maximum TOF of the fresh HB-Pd/C is around 4.33 hour^{-1}, higher than that of commercial Pd/C (2.85 hour^{-1}), AB-Pd/C (2.03 hour^{-1}), and CB-Pd/C (1.48 hour^{-1}). The reharvested AB-Pd/C lost nearly 70% of its activity with a maximum TOF of 0.57 hour^{-1} (Fig. 4B), and commercial Pd/C essentially lost all its activity (Fig. 4D). The loss of the catalytic activity in these two catalysts can be largely attributed to the seriously ripened nanoparticle size during the first cycle of catalytic reaction (see Fig. 3, F and H). In the case of HB-Pd/C and CB-Pd/C catalysts, because the nanoparticle size is largely unchanged during the first cycle of reaction, the recycled catalysts show much less change in catalytic activity (Fig. 3, E and G). Overall, the HB-Pd/C shows the highest initial catalytic activity, together with excellent recyclability (with the recycled catalytic activity twice that of CB-Pd/C and six times that of AB-Pd/C catalysts).

Our studies clearly demonstrate that different β-substitutions in the butyric acid ligands can greatly modulate the Ostwald ripening process and the catalytic activity and recyclability of the Pd nanoparticle catalysts, suggesting that the β-functional groups may play an important role in the catalytic cycle. Pd(0) sites on the particle surface have to be activated to Pd(II) by oxygen and acid to enter the catalytic cycle and enable the subsequent chemical transformation (Fig. 1). However, the Pd(II) ions may be easily leached off from the particle surfaces and lead to serious Ostwald ripening effects. The introduction of β-functional groups on butyric acid ligands could offer secondary binding sites to capture and anchor the Pd(II) ions on the particle surface and therefore prevent them from leaching into solution, thereby contributing to Ostwald ripening. In general, the stronger binding affinity of the β-functional groups, the tighter the Pd(II) ions are anchored on the surface, and the less the Ostwald ripening effect. However, too strong a binding ligand could also severely undermine the catalytic activity by competing with the substrate binding. Therefore, a proper binding strength of surface ligands to Pd(II) is essential for ensuring the optimized catalytic activity and stability.

Predicted by hard-soft acid base theory (HSABT) (*32*), the binding strength to Pd(II) follows a sequence of Cl > N > O. Thus, Cl is expected to have the strongest binding affinity to prevent Pd(II) from leaching off from the surface, and thus, CB-Pd/C exhibits minimum size change and the best recyclability during the catalytic reactions. X-ray photoelectron spectroscopy (XPS) studies show that there is significantly more proportion of Pd(II) in the nanoparticles after the catalytic reaction than the as-synthesized material (see fig. S4), indicating that a large portion of Pd is activated to Pd(II) and anchored on the nanoparticle surface. On the other hand, the tight binding of 3-chlorobutyric acid to Pd(II) can also partly passivate the catalytic activity with a compromised yield and TOF.

AB-Pd/C shows the most obvious Ostwald ripening during the catalytic reactions, which appears contradictory to a trend predicted by HSABT. To understand this fact, zeta potential measurements were performed. Zeta potentials of Pd nanoparticles with different ligands were measured before and after dispersion of the particles into a reaction solution, namely, DMSO solution containing TFA (Table 3). All particles show a positive shift of zeta potential after dispersing into the TFA/DMSO solution and washing process, which can be attributed to the partial protonation of the carboxyl group of all the three ligands by TFA. It is noted that the zeta potential of HB-Pd and CB-Pd remains negative after this process, whereas the AB-Pd zeta potential shifts from negative to positive, which can be attributed to the additional protonation of an amine

Table 2. The yield of various heterogeneous catalysts mediated for 3-methylcyclohexenone dehydrogenative oxidation. The reactions were carried out in 10 ml of dimethyl sulfoxide (DMSO) solutions containing 1 mmol of 3-methylcyclohexenone, 0.03 mmol of Pd-equivalent catalysts, and 1.2 mmol of TFA under 1 atm of oxygen at 100°C for 24 hours.

Entry	Catalyst	First-cycle yield (%)	Second-cycle yield (%)
1	HB-Pd/C	**93**	**83**
2	AB-Pd/C	74	24
3	CB-Pd/C	57	48
4	Commercial Pd/C	67	<1

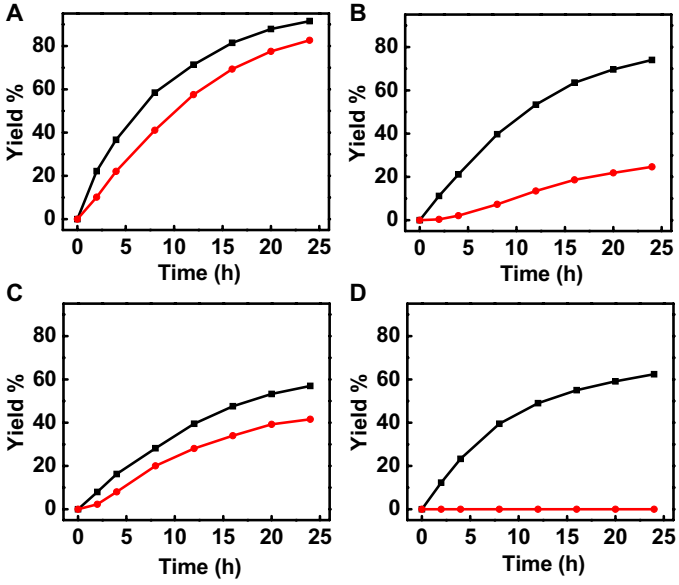

Fig. 4. Time-dependent reaction profiles of 3-methylcyclohexenone dehydrogenative oxidation. The black and red lines represent the reaction profiles catalyzed by the fresh and reharvested catalysts: (**A**) HB-Pd/C, (**B**) AB-Pd/C, (**C**) CB-Pd/C, and (**D**) commercial Pd/C.

Table 3. Zeta potential measurements on Pd nanoparticles before and after dispersing into a TFA/DMSO reaction solution.

Entry	Catalyst	Zeta potential (mV) (as prepared)	Zeta potential (mV) (after dispersing into reaction solution)
1	HB-Pd	−23.2	−2.79
2	CB-Pd	−21.6	−3.76
3	AB-Pd	−18.4	**2.41**

group to form positively charged NH_3^+. The protonation of AB greatly weakens its binding strength to Pd(II). Moreover, with a positive charge, the activated Pd(II) species could more likely be pushed away from the AB-Pd surface because of electrostatic repulsion from the positively charged NH_3^+, in contrast to an electrostatic attraction force in HB-Pd and CB-Pd. This process could greatly accelerate the Ostwald ripening of AB-Pd nanoparticles and result in reduced catalytic activity and poor recyclability, as we have seen in our experiments.

HB has a weaker binding strength to Pd(II) than CB but stronger than AB in the TFA solution. The ligation of HB prevents the activated Pd(II) from leaching into the solution and the Ostwald ripening thereof. The competition reaction of HB binding to Pd(II) is not significant compared to substrate binding because of its moderate binding strength, so that the activated Pd(II) could readily enter the catalytic cycle without passivation. The proper binding strength of HB is crucial for HB-Pd/C as a catalyst to simultaneously ensure little Ostwald ripening, outstanding stability, and excellent catalytic activity.

To further support the explanation using HSABT, we have further used 3-bromobutyric acid (BB) as a ligand to synthesized carbon-supported Pd nanoparticles (BB-Pd/C) and investigated their catalytic behavior (fig. S5). The synthesized Pd nanoparticles (BB-Pd/C) show a size similar to those obtained with the other ligands (10 nm; fig. S5A), indicating that the carboxyl group is still the dominating functional group in terms of particle formation. The catalytic reaction gave an even lower catalytic activity than CB-Pd/C (yield, 11%; fig. S5C) but with very good reharvestability (>95%; fig. S5C). This could attribute to a stronger binding affinity of a Br group (than Cl) to the Pd(II) due to the fact that Br is a softer base, which inhibits not only the Pd(II) leaching but also the catalysis. TEM studies also demonstrate that the particle sizes do not show any obvious change before and after the reaction (fig. S5B), which also support the explanation above.

CONCLUSION

In summary, by systematically engineering the ligands on the surface of Pd nanoparticle catalysts, we have created a highly active and stable heterogeneous catalyst for efficient aerobic reactions that greatly exceeds the activity of a homogeneous catalyst, especially under industry-favored high turnover conditions. The Pd nanoparticle heterogeneous catalysts could maintain undiminished activity, which is in contrast to homogeneous catalysts that typically suffer from deligation and decomposition to form large unreactive species that prevent the continuity of the reaction under high turnover conditions. Our systematic studies revealed that β-functional groups play a significant role for the high efficiency and robust characteristics of Pd nanoparticle catalysts by mediating catalytic cycles. Overall, our studies demonstrate a new strategy to design and develop heterogeneous catalysts for highly efficient chemical transformations. It can affect diverse areas, including synthetic methodology and green chemistry.

MATERIALS AND METHODS

Preparation of carbon-supported Pd nanoparticles capped with β-substituted butyric acid

The preparation of different β-substituted butyric acid–capped Pd nanoparticles followed the same process. In a typical synthesis, 625 μl of Na_2PdCl_4 stock solution (20 mM), 50 μl of ligand solution (20 mM), and 3.80 ml of H_2O were premixed in a glass vial by vigorous stirring. The $NaBH_4$ solution (50 mM) and ascorbic acid solution (50 mM) were freshly prepared each time before use. Ascorbic acid solution (0.05 ml) was first introduced into the reaction vial, followed by the injection of 20 μl of $NaBH_4$ solution. The final solution volume was 5 ml. The nanoparticles were allowed to grow for 20 min before being centrifuged and washed with water. The nanoparticles were then redispersed in 5 ml of water. The solution was then mixed with carbon black solution (isopropanol/water ratio of 3:2) for 10 min. The resulting mixture was centrifuged, washed with water and ethanol, and dried.

Aerobic dehydrogenative oxidation reaction conditions, recyclability, and time-dependent reaction kinetics

Typical aerobic dehydrogenative oxidation reactions were carried out in 10 ml of DMSO solutions containing 1 mmol of 3-methylcyclohexenone, 0.03 mmol of Pd-equivalent catalysts, and 1.2 mmol of TFA, under 1 atm of oxygen at 100°C for 24 hours. The reaction yield was determined via gas chromatography–mass spectrometry (GC-MS). The catalysts were centrifuged, washed with DMSO, and redispersed for recyclability tests. Time-dependent reaction courses were done by taking aliquots at each time interval and sampled by GC-MS.

SUPPLEMENTARY MATERIALS

Supplementary material for this article is available at http://advances.sciencemag.org/cgi/content/full/3/1/e1600615/DC1

fig. S1. FTIR spectrum of HB-Pd/C and HB.
fig. S2. TEM image of large particle formation after homogeneous $Pd(TFA)_2$-catalyzed reaction.
fig. S3. Hot filtration test of HB-Pd/C–catalyzed aerobic oxidation reaction.
fig. S4. XPS spectra of CB-Pd/C before and after reaction in Pd 3d region.
fig. S5. TEM morphology and size distribution of BB-Pd/C and catalytic behavior.

REFERENCES AND NOTES

1. Y. Li, J. H.-C. Liu, C. A. Witham, W. Huang, M. A. Marcus, S. C. Fakra, P. Alayoglu, Z. Zhu, C. M. Thompson, A. Arjun, K. Lee, E. Gross, F. D. Toste, G. A. Somorjai, A Pt-cluster-based heterogeneous catalyst for homogeneous catalytic reactions: X-ray absorption spectroscopy and reaction kinetic studies of their activity and stability against leaching. *J. Am. Chem. Soc.* **133**, 13527–13533 (2011).
2. Y. Wu, D. Wang, Y. Li, Nanocrystals from solutions: Catalysts. *Chem. Soc. Rev.* **43**, 2112–2124 (2014).
3. Y. Wang, S.-I. Choi, X. Zhao, S. Xie, H.-C. Peng, M. Chi, C. Z. Huang, Y. Xia, Polyol synthesis of ultrathin Pd nanowires via attachment-based growth and their enhanced activity towards formic acid oxidation. *Adv. Funct. Mater.* **24**, 131–139 (2014).
4. L. D. Pachón, G. Rothenberg, Transition-metal nanoparticles: Synthesis, stability and the leaching issue. *Appl. Organomet. Chem.* **22**, 288–299 (2008).
5. C.-Y. Chiu, Y. Li, L. Ruan, X. Ye, C. B. Murray, Y. Huang, Platinum nanocrystals selectively shaped using facet-specific peptide sequences. *Nat. Chem.* **3**, 393–399 (2011).
6. A. Dong, J. Chen, S. J. Oh, W.-k. Koh, F. Xiu, X. Ye, D.-K. Ko, K. L. Wang, C. R. Kagan, C. B. Murray, Multiscale periodic assembly of striped nanocrystal superlattice films on a liquid surface. *Nano Lett.* **11**, 841–846 (2011).
7. C. Wang, W. Tian, Y. Ding, Y.-q. Ma, Z. L. Wang, N. M. Markovic, V. R. Stamenkovic, H. Daimon, S. Sun, Rational synthesis of heterostructured nanoparticles with morphology control. *J. Am. Chem. Soc.* **132**, 6524–6529 (2010).
8. S. Xie, H.-C. Peng, N. Lu, J. Wang, M. J. Kim, Z. Xie, Y. Xia, Confining the nucleation and overgrowth of rh to the {111} facets of pd nanocrystal seeds: The roles of capping agent and surface diffusion. *J. Am. Chem. Soc.* **135**, 16658–16667 (2013).
9. J. Henzie, S. C. Andrews, X. Y. Ling, Z. Li, P. Yang, Oriented assembly of polyhedral plasmonic nanoparticle clusters. *Proc. Natl. Acad. Sci. U.S.A.* **110**, 6640–6645 (2013).
10. D. Zaramella, P. Scrimin, L. J. Prins, Self-assembly of a catalytic multivalent peptide–nanoparticle complex. *J. Am. Chem. Soc.* **134**, 8396–8399 (2012).
11. M. Tamura, H. Fujihara, Chiral bisphosphine BINAP-stabilized gold and palladium nanoparticles with small size and their palladium nanoparticle-catalyzed asymmetric reaction. *J. Am. Chem. Soc.* **125**, 15742–15743 (2003).
12. T. Mitsudome, T. Umetani, N. Nosaka, K. Mori, T. Mizugaki, K. Ebitani, K. Kaneda, Convenient and efficient Pd-catalyzed regioselective oxyfunctionalization of terminal olefins by using molecular oxygen as sole reoxidant. *Angew. Chem. Int. Ed.* **118**, 495–499 (2006).

13. T. Mitsudome, K. Mizumoto, T. Mizugaki, K. Jitsukawa, K. Kaneda, Wacker-type oxidation of internal olefins using a $PdCl_2$/*N*, *N*-dimethylacetamide catalyst system under copper-free reaction conditions. *Angew. Chem. Int. Ed.* **49**, 1238–1240 (2010).
14. A. N. Campbell, P. B. White, I. A. Guzei, S. S. Stahl, Allylic C–H acetoxylation with a 4,5-diazafluorenone-ligated palladium catalyst: A ligand-based strategy to achieve aerobic catalytic turnover. *J. Am. Chem. Soc.* **132**, 15116–15119 (2010).
15. J. H. P. Tyman, *Synthetic and Natural Phenols* (Elsevier, New York, 1996).
16. K. M. Gligorich, M. S. Sigman, Recent advancements and challenges of palladium^{II}-catalyzed oxidation reactions with molecular oxygen as the sole oxidant. *Chem. Commun.* **2009**, 3854–3867 (2009).
17. C. S. Yi, D. W. Lee, Efficient dehydrogenation of amines and carbonyl compounds catalyzed by a tetranuclear ruthenium-μ-oxo-μ-hydroxo-hydride complex. *Organometallics* **28**, 947–949 (2009).
18. J. Muzart, J. P. Pete, Dehydrogenation of cyclohexanones catalyzed by palladium(II) trifluoroacetate. *J. Mol. Catal.* **15**, 373–376 (1982).
19. J. Muzart, One-pot syntheses of α,β-unsaturated carbonyl compounds through palladium-mediated dehydrogenation of ketones, aldehydes, esters, lactones and amides. *Eur. J. Org. Chem.* **2010**, 3779–3790 (2010).
20. D. R. Buckle, in *Encyclopedia of Reagents for Organic Synthesis*, D. Crich, Ed. (Wiley, New York, 2010).
21. Y. Izawa, D. Pun, S. S. Stahl, Palladium-catalyzed aerobic dehydrogenation of substituted cyclohexanones to phenols. *Science* **333**, 209–213 (2011).
22. Z. Lu, S. S. Stahl, Intramolecular Pd(II)-catalyzed aerobic oxidative amination of alkenes: Synthesis of six-membered *N*-Heterocycles. *Org. Lett.* **14**, 1234–1237 (2012).
23. D. Pun, T. Diao, S. S. Stahl, Aerobic dehydrogenation of cyclohexanone to phenol catalyzed by $Pd(TFA)_2$/2-dimethylaminopyridine: Evidence for the role of Pd nanoparticles. *J. Am. Chem. Soc.* **135**, 8213–8221 (2013).
24. M. Sutter, N. Sotto, Y. Raoul, E. Métay, M. Lemaire, Straightforward heterogeneous palladium catalyzed synthesis of aryl ethers and aryl amines via a solvent free aerobic and non-aerobic dehydrogenative arylation. *Green Chem.* **15**, 347–352 (2013).
25. M. Sutter, M.-C. Duclos, B. Guicheret, Y. Raoul, E. Métay, M. Lemaire, Straightforward solvent-free heterogeneous palladium-catalyzed synthesis of arylamines from nonaromatic substrates by dehydrogenative alkylation. *ACS Sustain. Chem. Eng.* **1**, 1463–1473 (2013).
26. J. Zhang, Q. Jiang, D. Yang, X. Zhao, Y. Dong, R. Liu, Reaction-activated palladium catalyst for dehydrogenation of substituted cyclohexanones to phenols and H_2 without oxidants and hydrogen acceptors. *Chem. Sci.* **6**, 4674–4680 (2015).
27. K. R. Gopidas, J. K. Whitesell, M. A. Fox, Synthesis, characterization, and catalytic applications of a palladium-nanoparticle-cored dendrimer. *Nano Lett.* **3**, 1757–1760 (2003).
28. T. Fang, K. Ma, L. Ma, J. Bai, X. Li, H. Song, H. Guo, 3-Mercaptobutyric acid as an effective capping agent for highly luminescent CdTe quantum dots: New insight into the selection of mercapto acids. *J. Phys. Chem. C* **116**, 12346–12352 (2012).
29. L. Ruan, H. Ramezani-Dakhel, C.-Y. Chiu, E. Zhu, Y. Li, H. Heinz, Y. Huang, Tailoring molecular specificity toward a crystal facet: A lesson from biorecognition toward Pt{111}. *Nano Lett.* **13**, 840–846 (2013).
30. G.-J. ten Brink, I. W. C. E. Arends, R. A. Sheldon, Green, catalytic oxidation of alcohols in water. *Science* **287**, 1636–1639 (2000).
31. R. A. Sheldon, I. W. C. E. Arends, G.-J. ten Brink, A. Dijksman, Green, catalytic oxidations of alcohols. *Acc. Chem. Res.* **35**, 774–781 (2002).
32. J. D. Hoeschele, J. E. Turner, M. W. England, Inorganic concepts relevant to metal binding, activity, and toxicity in a biological system. *Sci. Total Environ.* **109–110**, 477–492 (1991).

Acknowledgments

Funding: Y.H. acknowledges the support from the Office of Naval Research through award N00014-15-1-2146 (nanocatalyst synthesis). X.D. acknowledges the support from the U.S. Department of Energy, Office of Basic Energy Sciences, Division of Materials Sciences and Engineering through award DE-SC0008055 (nanocatalyst characterization and catalytic studies). **Author contributions:** X.D. and Y.H. designed the experiments and supervised the research. T.X. and Z.L. carried out the experiments and performed the data analysis. All other authors contributed to material characterization and product analysis. All authors discussed the results and commented on the manuscript. **Competing interests:** The authors declare that there are no competing interests. **Data and materials availability:** All data needed to evaluate the conclusions in the paper are present in the paper and/or the Supplementary Materials. Additional data related to this paper may be requested from the authors by emailing X.D. at xduan@chem.ucla.edu and Y.H. at yhuang@seas.ucla.edu.

Submitted 23 March 2016
Accepted 21 November 2016
Published 6 January 2017
10.1126/sciadv.1600615

Citation: T. Xue, Z. Lin, C.-Y. Chiu, Y. Li, L. Ruan, G. Wang, Z. Zhao, C. Lee, X. Duan, Y. Huang, Molecular ligand modulation of palladium nanocatalysts for highly efficient and robust heterogeneous oxidation of cyclohexenone to phenol. *Sci. Adv.* **3**, e1600615 (2017).